J. ISSS Vol. **1** No. 1, pp. 55-64, Sept 2012.
REGULAR PAPER

Design, Fabrication and Characterization of RF MEMS Varactor for VCO Application

Sukomal Dey[1a] and Shiban.K.Koul[a]
[a]RF and Microwave Laboratory, Centre for Applied Research in Electronics (CARE)
Indian Institute of Technology, Delhi
[1a]sdey_care@rediffmail.com
[a]shiban_koul@hotmail.com

Keywords:
MEMS,
Varactor,
VCO,
Capacitance tuning ratio,
Pull-in, SEM,
Vibration spectrum,
LDV

Abstract

A tunable capacitor that employs micro electromechanical systems (MEMS) based on the electostatically actuated parallel plate concept and suitable for Voltage Controlled Oscillators (VCO) at RF frequencies is presented in this paper. The main objective of this work is to achieve a frequency tuning capability of high quality. The dimensions of the MEMS device have been optimized with the Finite Element Method based CoventorWare analysis software and verified through a lumped parameter analysis in a Saber platform. The varactor has been fabricated using gold-based surface micromachining process. Both the mechanical and electrical performance of the device have been verified using a lumped parameter analysis in a Saber platform. The mechanical response, electrical response and loss performance of the varactor have been experimentally investigated.

1. Introduction

The Micro-electromechanical Systems (MEMS) technology is primarily used to develop miniaturized, integratable, high quality factor (Q) frequency selective circuits. High-Q devices are fundamental for different passive and active circuits and can substantially reduce the phase noise or power consumption of oscillators and amplifiers [Rebeiz, 2003]. The Voltage Controlled Oscillator (VCO) at RF frequency is composed of the CMOS circuit and the LC tank in the conventional negative-gm topology. So, the capacitance change in the MOS capacitor limits the tuning range and the operating frequency of the VCOs and the nonlinearity of the tuning devices degrade the phase noise of the RF VCOs [Dec and Suyamma, 2000]. The MEMS tuneable capacitors have been shown to give out adequate quality when they are fabricated using either aluminium or silicon or gold surface micromachining technology. These devices are expected to offer an excellent linearity since they do not respond to high frequencies outside their mechanical resonance frequencies [Dec and Suyamma, 1998a]. The tunability of the VCOs depends on the tuning range of the capacitors in the tank circuits. Lesson's formula of the phase noise of a VCO describes the inverse square relationship between the phase noise and the Q-factor of the tank circuit [Dec and Suyamma, 1998b]. From that, it is evident that phase noise performance can be improved by increasing the Q- factor of the tank circuit. Since on-chip inductors do not give very high Q values, the Q-factor of the varactor device needs to be increased. On-chip MOS varactors are very difficult to realize with low phase noise and high quality factors that can sustain a wide process and temperature variation [Nieminen *et al*., 2004]. A MEMS based varactor is therefore a good replacement of the on-chip MOS varactors in this regard. Due to low loss, the MEMS varactor possesses the property of very high Q values and is capable of withstanding wide process

and temperature variations. In addition, conventional micro-machined tuneable capacitors [Mc Corquodale *et al*., 2002] are not expected to respond to RF frequencies in the 1–2 GHz range especially since their mechanical resonant frequencies normally lie in the 10–100 kHz. Therefore, with RF frequencies 10,000 times the mechanical bandwidth, these devices are unlikely to produce a significant amount of harmonic content [O'Mahony *et. al*, 2003]. The main limitation of these devices, however, has been the fact that their tuning ranges thus far have been less than theoretical calculations suggested [Fedder and Mukherjee, 2005]. In this paper, the design optimization and simulation of a two parallel plate variable capacitor for VCO applications using the method of electrostatic actuation is presented. Suspension beams have been optimized for 3.3Volt VCO power supply. The working principal is derived from changing the gap between two parallel plates using electrostatic actuation; one is fixed on the substrate and other one is suspended with four T-shaped suspension beams.

The layout of this paper is as follows. Section II presents modeling and optimization issues including the computation of spring constants and the Q-factor analysis. Section III presents detailed electromechanical simulation along with the capacitance variation of the two plate varactor. Optimization of the capacitor dimensions have been achieved using CoventorWare simulation software. The electro-mechanical lumped parameter representation of the same has been realized in the Saber platform. Section IV, describes the fabrication process of the RF MEMS varactor and Section V describes mechanical, electrical and RF response of the MEMS varactor.

2. Modelling and design optimization of mems varactor

2.1 Design Consideration

The electromechanically tunable capacitor consists of two parallel plates, four T-shaped suspension beams to suspend the top plate as shown in Fig. 1. The top plate is pulled down to the bottom plate with electrostatic force.

The dynamics of an electromechanical two plate varactor can described expressed by [Rebeiz, 2003]

$$m\frac{d^2x(t)}{dt^2}+b\frac{dx(t)}{dt}+kx(t)=\frac{1}{2}\frac{dc_d(t)}{dx}V_1^2(t) \quad (1)$$

where m is the mass of the suspended plate, b is the mechanical resistance, k is the effective spring constant, C_d is the desired capacitance and V_1 is the applied electrostatic potential between the two parallel plates. The current flowing through the desired capacitance is given by [Rebeiz, 2003]

$$i(t)=C_d(t)\frac{dv_1(t)}{dt^2}+V_1(t)\frac{dC_d(t)}{dt} \quad (2)$$

The suspended plate moves towards the fixed plate until a point of instability occurs where the electrostatic force becomes exactly equal to the spring restoring force, corresponding to a 50% capacitance increase. The equilibrium between the forces can be written mathematically as given by (3).

$$kx=\frac{1}{2}\frac{dc_d}{dx}V_1^2=-\frac{1}{2}\frac{\varepsilon_d A V_1^2}{(d_1-x)^2} \quad (3)$$

where x is the displacement under dc conditions, $\varepsilon_d$is the dielectric constant of air ($\varepsilon_d = \varepsilon_{air}\varepsilon_0$, where ε_{air}=1.00054 and ε_0= 8.854 × 10^{-12} F/m), A is the overlapping area of the two parallel plates, and d_1 is the separation of the capacitor plates when the spring is in its relaxed state.

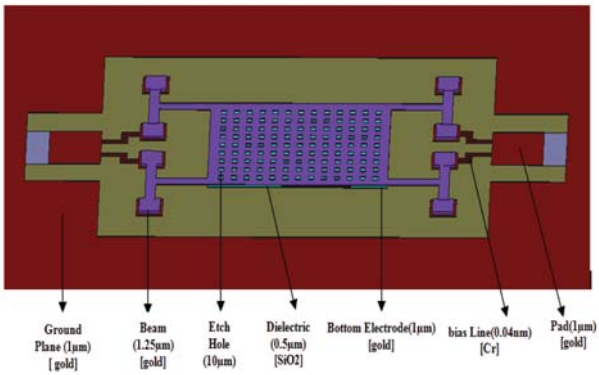

Figure1: Schematic illustration of a variable capacitor on substrate

In theory, the suspended plate can be pulled down at most by 1/3 of the original gap, so the maximum capacitance that can be tuned to is $3C_d/2$, and the maximum theoretical tuning range would be 1.5:1 as shown in (4)

$$\text{Tuning Ratio(TR)} = \frac{C_{max}}{C_{min}} = \frac{\varepsilon A/(2x/3)}{\varepsilon A/x} = 1.5 \quad (4)$$

Incorporating a worst-case-scenario fringing capacitance (C_f) of 40% of C_{max} the value of the capacitance tuning ratio is obtained by

$$TR = \frac{C_{max} + 0.4C_{max}}{C_{min} + 0.4C_{max}}, \text{ since } C_{max} = 1.5C_{min} \quad (5)$$

A semi-analytical model of the pull-in voltage can be obtained from [McCorquodale *et al*.2002] which calculates the total potential energy content of a fixed-fixed beam subject to electrostatic actuation without considering the fringing field effects. A correction factor is then applied to account for the fringing field effects. The first-order fringing field effects have been approximately compensated for by an effective beam width. Following [16], the pull-in voltage can be obtained as given in (6)[O' Mahony *et al*., 2003]

$$V_{PI} = \sqrt{\frac{1}{\left(1+0.65\frac{x}{w}\right)}} \times \sqrt{\frac{c_1 E h^3 x^3}{\varepsilon_0 l^4} + \frac{c_2(1-\nu)x_0 h \sigma_0}{\varepsilon_0 l^2}} \quad (6)$$

ε_0

The constants are c_1 =11.7 and c_2 =3.6, E is Young's modulus and õ is Poisson's ratio, x is the gap between the two parallel plates, *l* and *h* are the beam length and width respectively, *w* is the thickness of the beam and is the permittivity of free space.

C_0 is the original capacitance without applying voltage or RF signal and K_m is the effective spring constant of the four T-shaped beams, which can be written as (7)

$$K_m = 4K_{eq},\ K_{eq} = \frac{k_1 2k_2}{k_1 + 2k_2},\ k_i = \frac{Ew_i T_i^3}{L_i^3} \quad (7)$$

K_{eq} is the equivalent spring constant of each T-shaped beam, L_i, W_i and T_i are the length, width and thickness of the beams and E is Youngs Modulus of the material.

2.2 Quality factor analysis

Various sources of loss can affect the quality at high frequency. In our design the two-plate varactor is modeled with conductive and resistive plates. This is justified in our case where the top plate is deposited with gold and the bottom plate is made up with gold coated with silicon-dioxide.

The expression of the quality factor of the varactor which can be obtained from the input admittance of the varactor, is given by (8) [McCorquodale *et al*., 2002]

$$\frac{Q+1}{Q-1} = \frac{\sin\left(\sqrt{2\omega\tau}\right) + 2\cos\left(\sqrt{\frac{\omega\tau}{2}}\right)\sin\left(\sqrt{\frac{\omega\tau}{2}}\right)}{\sinh\left(\sqrt{2\omega\tau}\right) + 2\sinh\left(\sqrt{\frac{\omega\tau}{2}}\right)\cos\left(\sqrt{\frac{\omega\tau}{2}}\right)} \quad (8)$$

Where τ is the time constant of the varactor that is expressed by (9)

$$\tau = R_P C_D \quad (9)$$

where R_P is the resistance of the resistive plate (i.e sheet resistance for a square plate capacitor), C_D is the total capacitance between the two parallel plates and w is the operating frequency in radian. Since the losses due to interconnects and the substrate parasitic are not considered in our design, the expression presented above represents the maximum theoretically achievable Q-factor. The above expression represents the maximum theoretically achievable Q-factor. At 1.9 GHz, and 2.4 GHz the calculated Q-factors are 460 and 381respectively, which suggests that a high -factor can be achieved in this process.

3. Electromechanical modelling of a varactor with parametric optimization

The varactor structure, as shown in Fig.1, consists of a centrally placed rectangular gold proof-mass which is suspended with four symmetrically

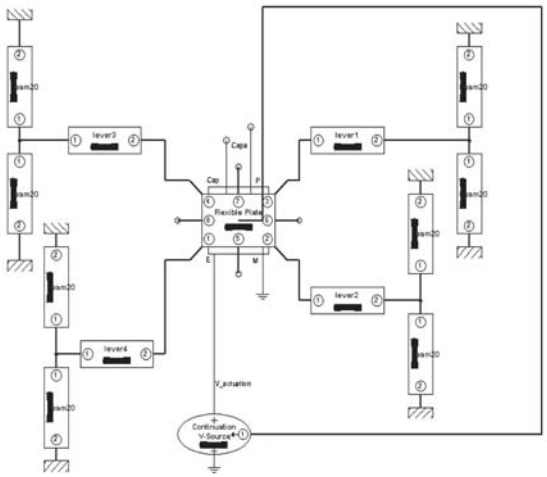

Figure 2. System model of the MEMS varactor in Saber

placed T-shaped suspension gold beams; two are on one side and two on the other. All the beams are rigidly clamped from two fixed walls on each side. Also, there is a gold electrode placed underneath the proof-mass along with a dielectric layer with an air gap of 2.5 μm. The behavioural analysis and electromechanical modelling have been carried out in a Coventorware platform.

To realize the MEMS varactor model in Saber software, parallel conductor plates and clamped beams have been clubbed together and assigned with a particular point as a knot in the 3- dimensional space shown in Fig.2.

In our design, a T-type suspension beam has been modelled to operate the varactor with a 3.3 Volt DC power supply. With this applied voltage the varactor can be used in the LC tank circuit in the VCO at RF frequencies. The lever length (ll) and lever width (lw) of the RF MEMS two plate varactor have been optimized with lumped parameter modelling. The lever length(ll) is varied from 60μm to 120μm and the lever width (lw) is varied from 20μm to 50μm in steps of 10μm. A small signal ac analysis, and pull-in voltage and capacitance variation have been carried out through lumped parameter modelling in a Saber platform and verified with FEM based simulation as shown in Figures 4 to Fig 11.

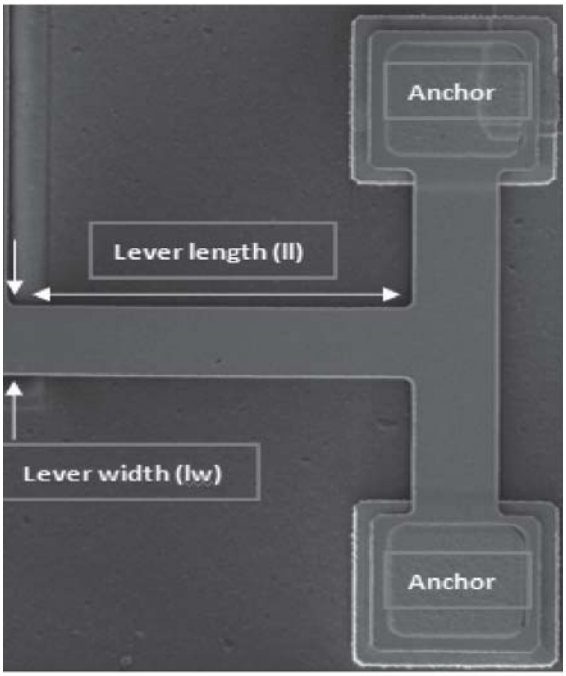

Figure 3. SEM image of T-shaped suspension beam

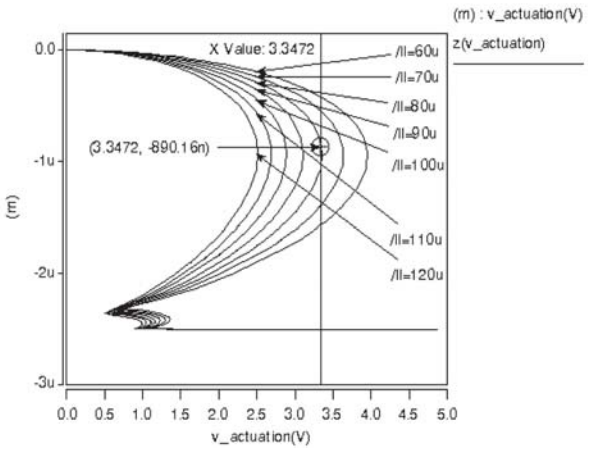

Figure 4. Pullin voltage analysis with parametric variation of Lever length (ll) where lever width(lw) is 20μm

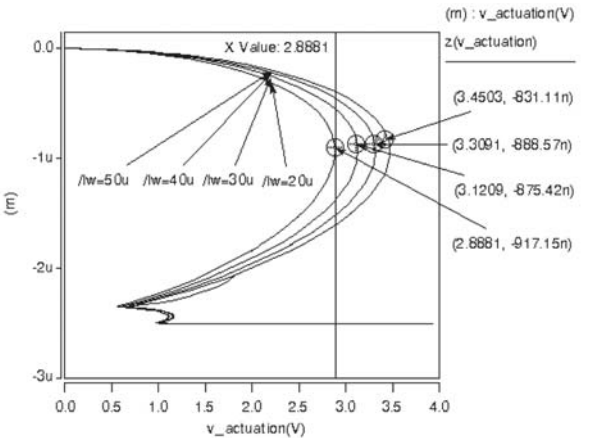

Figure 5. Pullin voltage analysis with parametric variation of Lever width (lw) where lever length(ll) is 100μm.

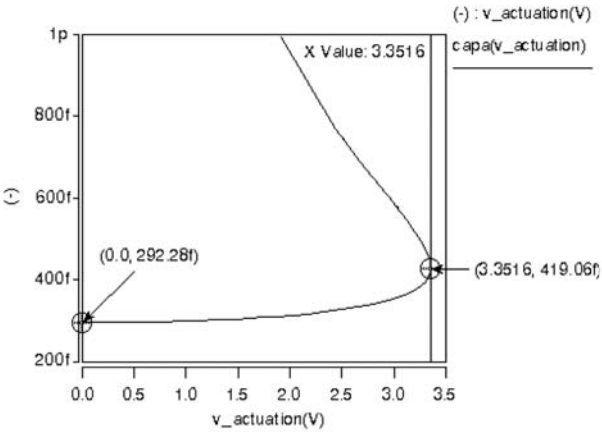

Figure 6. Capacitance variation with applied bias with 80μm lever length and 20μm lever width.

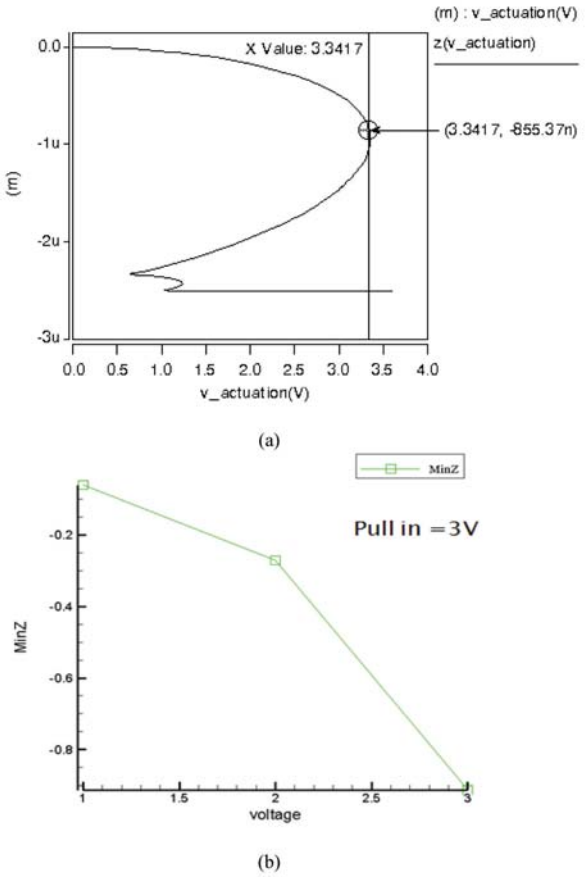

Figure 7. Variation of gap with applied bias; lever length = 80µm and lever width= 20µm (a) SABER based (b) FEM based, simulation.

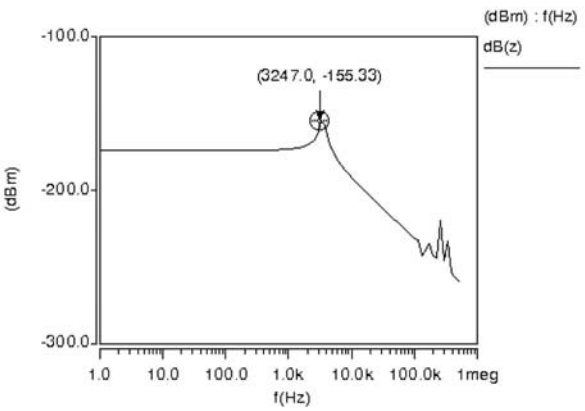

Figure 8. Fundamental mode of vibration of RF MEMS varactor with 80µm lever length and 20µm lever width.

FEM-based simulation shows that the point of instability occurs exactly at 1/3 of the gap (0.833 µm) from the top (2.5/3) with a voltage of 3 volts.

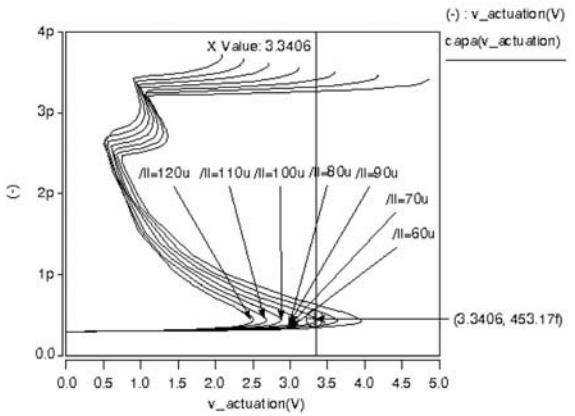

Figure 9. Capacitance Variation with lever length (ll) where lever width(lw) is 20µm.

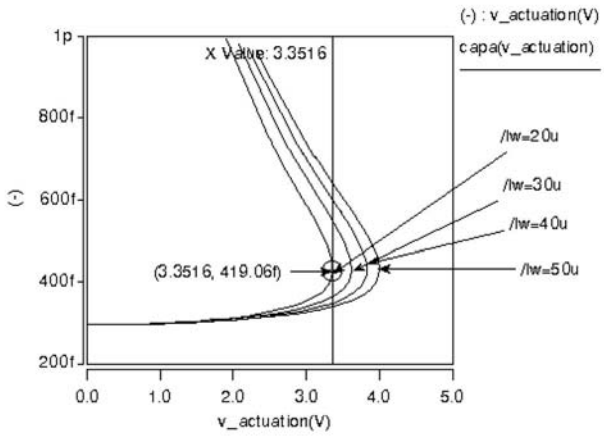

Figure 10. Capacitance Variation with Lever width (lw,) where lever length(ll) is 80µm.

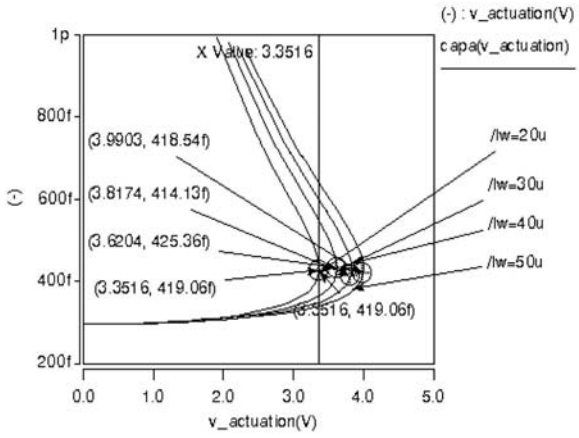

Figure 11. Variation of Tuning Ratio(TR) with the optimization of Lever width (lw)

Furthermore, an analytical pull-in voltage of 3.8volt was obtained from equation (6), after parametric optimization.

The fundamental mode of vibration of the varactor is 3.24 KHz (Fig. 8) after parametric optimization. The pull-in voltage is set to 3.3 Volts after the parametric variation. Tuning Ratio (TR) of this varactor is set to 1.433 after optimization as shown in Fig.6. So, 80μm lever length and 20μm lever width has been chosen for our design to actuate the varactor with 3.3Volts. The final design parameter of the MEMS varactor is listed in Table I as shown below.

Table 1: Dimensions of a two plate varactor

No	Two plate varactor	
	Parameter	**Dimensions (μm)**
1	Substrate	700 × 700 × 625
2	Actuation electrode	350 × 250 × 1
3	Dielectric	370 × 270 × 0.5
4	Proof mass	350 × 250 × 1.25
5	Beam	80 × 20 × 1.25
6	Air gap	2.5
7	Number of beams	4

4. Micro-fabrication of RF MEMS varactor

The fabrication process of the MEMS Varactor starts with a 0.025" thick Alumina substrate polished on both sides. The relative permittivity of the substrate is 9.8 with a loss tangent of 0.0001 at 1MHz. The masks that are used for the process are E-beam-write chrome masks. The alumina substrate is used in this work because of its following properties

- Good mechanical strength
- Good heat conductivity and fire resistance
- Good corrosion and wear resistance
- Very good electric insulation
- Good surface with high smoothness and less porosity
- Stability at very high temperatures and corrosive chemical

The fabrication process requires six masks and involves the following steps as shown in Fig. 12.

Step1. After the RCA cleaning of the wafer, the first layer of chromium (Cr) is deposited and patterned using the lift-off technique. This layer is used to make electrical biasing in the circuit by mask 1.

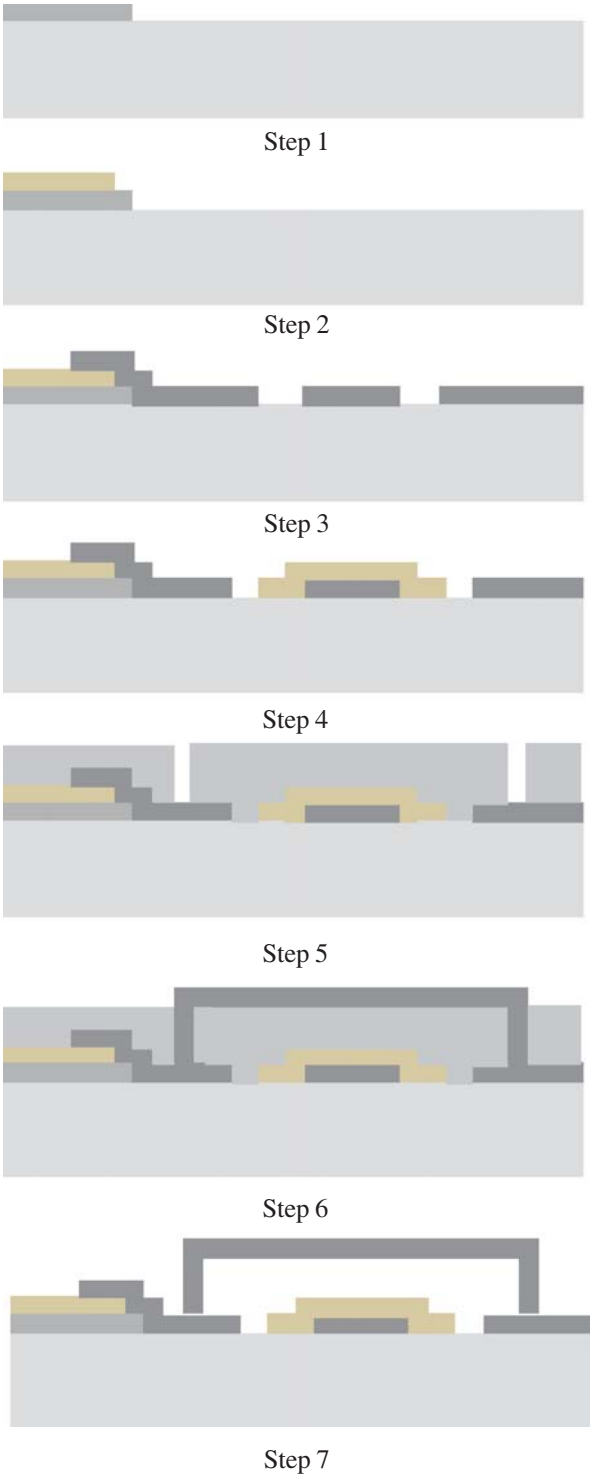

Figure12. Schematic view of micro- fabrication process steps.

Step2. 0.3 μm of Silicon Oxide (SiO_2) is deposited using plasma enhanced chemical vapour deposition (PECVD) and patterned. RIE is employed to pattern the oxide and remove the patterning photo resist. This is a passivation layer and deposited on the last layer (Cr) by mask 2. The

sheet resistance of this layer is 0.025 Ω/sq.

Step3. An evaporated 400Å chromium/100nm gold bilayer is deposited as a seed layer. A photo-resist mould is formed in the third lithographic step and 1ìm gold is electroplated inside the mould. The mould and seed layers will be removed afterwards. The chromium is applied as an adhesion layer for the gold. This layer used to pattern the CPW line, fixed electrodes and bias pad by mask 3.

Step4. 300Å of Titanium Tungsten (TiW) film is sputtered and followed by the deposition of 0.5µm silicon oxide using PECVD at 250°C. The dielectric and TiW layers are dry etched. The TiW layer serves as an adhesion layer for the silicon oxide to the gold. This layer is patterned by mask 4 to make an insulation layer on the CPW line and on actuation electrodes.

Step5. Spin coated Polyimide (PI) is used as a sacrificial layer for this process. Initially, it is coated to a thickness of 2.5ìm. Next, it is patterned by mask 5 (anchor mask) in an RIE step to etch the PI and fully clear the anchor holes.

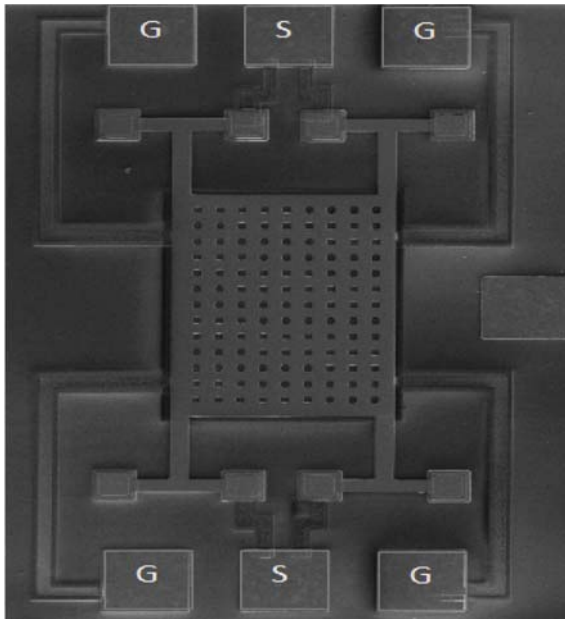

Figure13. Micro-fabricated image of MEMS varactor

Step6. The top gold layer consists of a sputtered gold seed layer and electroplated gold. The total thickness of this layer is 1.25µm, and it is used as the structural layer for the devices. A moulding method is used to define this layer. This layer is patterned to make a mobile electrode by mask 6. The sheet resistance of this layer is 0.02 Ω/sq. The density of this electroplated gold is 19300 kg/m^3.

Step7. The final step is the release process. In this process, the sacrificial layer is removed in an oxygen plasma dry etch process.

Micro-fabricated images of the MEMS varactor are shown in Fig. 13. The material properties are listed in Table II.

Table 2 : Dimensions of a two plate varactor

No	Material Properties of a fabricated MEMS varactor	
1	Young's Modulus of gold	45 GPa
2	Conductivity of gold	4.1 e^7 S/m
3	Sheet resistance of bottom gold electrode	0.025Ù square
4	Sheet resistance of top gold electrode	0.02 Ù/ square
5	Poisson ratio of gold	0.4
6	Density of gold	19300Kg/m^3

5. Testing and characterization of mems varactor

Mechanical and electrical tests have been performed on the varactor to examine the characteristics of the structure. The voltage actuation method has been used to detect the mechanical vibrations of the varactor. A small signal frequency sweep has been imposed over a dc actuation voltage to observe the frequency response of the particular structure. The out-of-plane vibration amplitude response has been recorded for the frequencies of the signal. A Polytec made Laser Doppler Vibrometer (LDV) has been used to detect the displacement of the structure in the out-of-plane direction. The LDV uses the Doppler frequency shift method to calculate displacement due to external excitation at the point where the laser pointer is focused.

The vibration spectrum of the MEMS varactor with applied external excitation has been shown in Fig.14(a). The first mode of vibration of the structure at 1.475 kHz which is obtained from the LDV is given in Fig.14(b)

The variation of capacitance with the actuation voltage of the structure has been performed using a DC probe station manufactured by Sus-Microtec,

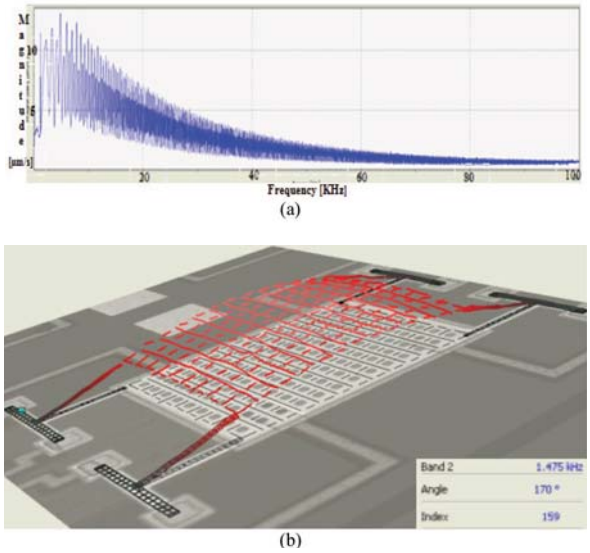

Figure14. (a) Vibration spectrum of the MEMS varactor (b) First mode of vibration

a DC voltage source and an LCR meter manufactured by Agilent. To measure the C-V characteristics, the bottom fixed plate of the varactor has been grounded and the required voltage sweep from 0 volt to 2.5volt has been applied to the top suspended electrode using the probes. A small AC signal of 5MHz has been imposed on the DC actuation voltage to measure the capacitance. Open circuit offset measurement corrections were made before recording the capacitance values. The capacitance of the varactor with a change in voltage has been observed and plotted by the LCR meter as shown in Fig.15. The steps in the measured capacitance value are due to the asymmetry of the suspended electrode over the fixed bottom electrode. The asymmetry is due to the initial deformation of the top plate along with the bending motion of the T-shaped suspension beam.

From the measured capacitances, the minimum and maximum capacitances available from the device are 0.86pF and 0.896pF respectively. The measured capacitance tuning ratio of the varactor is about 1.06:1 (%6). The measured tuning ratio of the experimental device is lower than the designed values. The parasitic capacitance of the pads (G-S-G) [Fig.13] along with the substrate capacitance affects the tuning range significantly and this was not considered during the simulation. Furthermore, residual stress in the suspended plate produces a warping of the capacitor plates, which effectively results in a different plate separation and, thus, a different parallel-plate capacitance, which

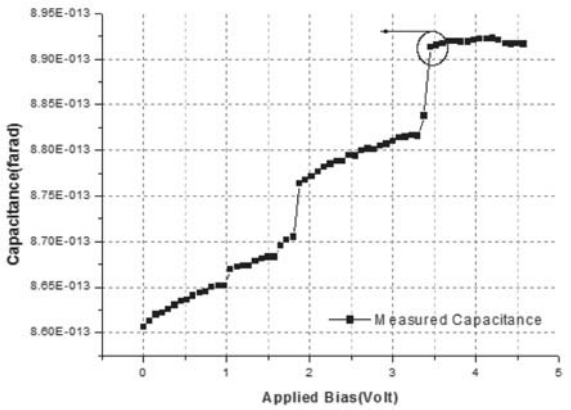

Figure15. Measured capacitance variation with applied voltage, Circle indicates the point of instability (pull-in) at 3.3Volt

leads to an effect on the tuning ratio. Moreover, measurements were carried out in air ambient conditions where air is used as a dielectric for the tunable capacitor, and its properties as a function of pressure, temperature, and humidity must be examined. The tunable capacitor may be operated in a vacuum, which resolves many issues that can arise when air is used as a dielectric. For example, the mechanical resistance can be dramatically reduced, and hence the mechanical Q-factor can be significantly improved when the tunable capacitor is placed in the vacuum. In addition, the mechanical noise due to the thermal agitation of air molecules can be reduced as mechanical resistance is reduced. Furthermore, there is no dielectric breakdown in the vacuum.

The loss measurement of the varactor was carried out using Vector Network Analyser. The measured varactor is connected with the series path of the transmission line. A return loss better than 18.17 dB and 16.46 dB with an insertion loss of 0.77dB and 0.83dB was obtained at 1.9 GHz and 2.4 GHz respectively as shown in Fig.16.

Return loss and insertion loss values are given at two different oscillation frequencies of the VCO; 1.9GHz and 2.4GHz. Quality factor has been obtained from measured S-parameter data (S_{11}) as given in (10).

$$Q = \frac{2|\mathrm{Im}(S_{11})|}{1-|S_{11}|^2} \qquad (10)$$

The variation of the Quality factor with frequency is shown in Fig17 which is obtained from

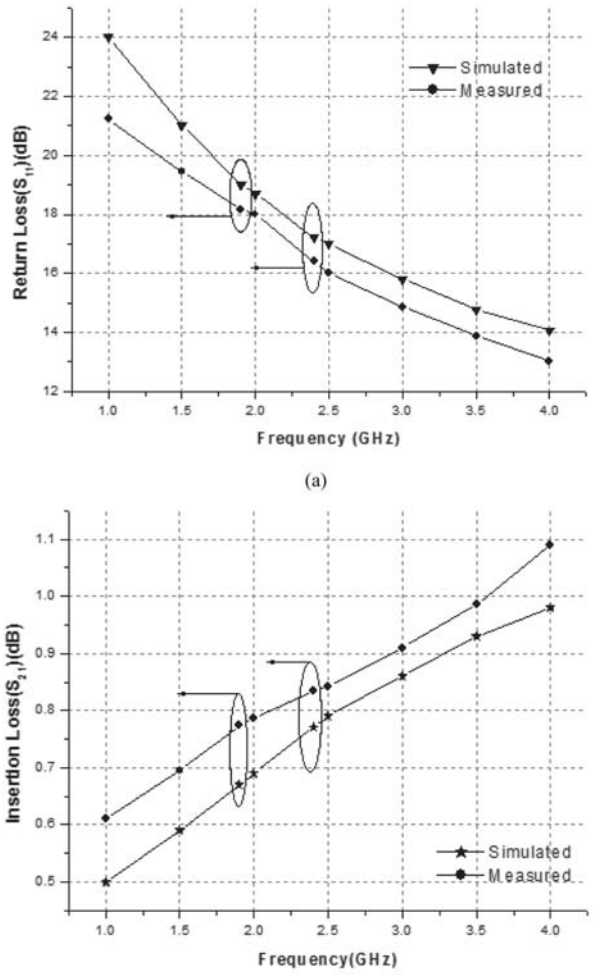

Figure16. (a) Return loss (b) Insertion Loss. Circles indicate return loss and insertion loss values at 1.9GHz and 2.4GHz.

equation (10) with measured return loss data. The Performance table of the micro-machined tunable capacitor is given in Table III.

6. Conclusions

This paper presents the development of a MEMS varactor including design, simulation, fabrication process and functional testing. A comparison between the simulated and tested results is also reported. The fundamental mode of vibration from LDV measurements is found within 15% tolerance from the simulation results. The variation in the value is quite acceptable as test conditions include unavoidable environmental perturbations, and damping and process variations which are not considered in the simulation. Also, the variation of capacitance with actuation voltage as obtained from testing and depicted in Fig.15 shows that the capacitance tuning ratio of the

Table 3: Performance of a two plate varactor

No	Performance of a fabricated MEMS varactor			
	Para-meters	Analy-tical	Simu-lated	Meas-ured
1	Pull-in voltage (volt)	3.8	3.34	3.3
2	Mode frequency (KHz)	-	3.24	1.475
3	Tuning ratio	1.5:1	1.4:1	1.06:1
4	S_{11} (dB) @ 1.9 GHz	-	19.5	18.17
5	S_{11} (dB) @ 2.4 GHz	-	17.54	16.46
6	S_{21} (dB) @ 1.9 GHz	-	0.6	0.77
7	S_{21} (dB) @ 2.4 GHz	-	0.74	0.83
8	Q-factor @ 1.9 GHz	460	391	360
9	Q-factor @ 2.4 GHz	381	301	280

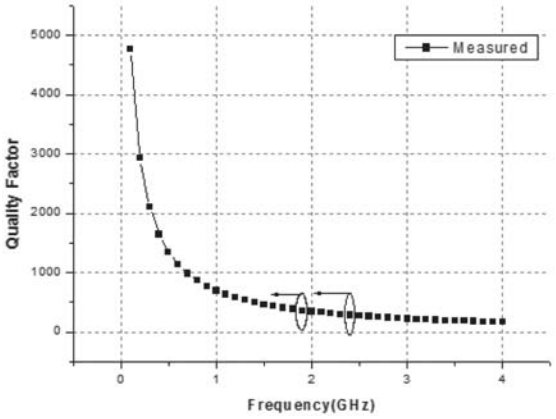

Figure17. Variation of quality factor with frequency, circles indicates quality factor value at 1.9GHz=360 and at 2.4GHz=280.

varactor is about 1.06:1. The sudden change in the measured capacitance at around 3 volts manifests the pull-in condition. The loss performance and the quality factor are quite acceptable over the desired frequency range for VCO applications.

Acknowledgments

We are grateful to the National Programme on Micro and Smart Systems (NPMASS) for setting up RF Characterization facilities and the MEMS Design Centre at the Indian Institute of Technology, Delhi. We would also like to thank Prof. Vijay Misra, Prof. Navakanta Bhatt and their group members for their support and help in performing the characterization at CEN, IISc, Bangalore.

References

Dec, A. and Suyama, K., 1998, Micromachined electro-mechanically tunable capacitors and their applications to RF IC's, IEEE Transaction on Microwave Theory & Techniques, 46: 2587-2596.

Dec, A. and Suyama, K., 1998b, RF micromachined varactor with wide tuning range, IEEE Radio Frequency Integrated Circuits Symposium Digest, 1: 309-312.

Dec, A. and Suyama, K., 2000, Microwave MEMS-based voltage-controlled oscillators, IEEE Transaction on Microwave Theory & Techniques, 48: 1943-1949.

Fedder, G., and Mukherjee, T., 2005, Tunable RF and analog circuits using on-chip MEMS passive components, in Digest of Technical Papers, IEEE Solid-State Circuits Conference, ISSCC. Feb. 2005, 390-391.

McCorquodale, M.S., Ding M.K., and Brown, R.B., 2003, A CMOS voltage-to-frequency linearizing preprocessor for paralie1 plate RF MEMS varactors, IEEE Radio Frequency Integrated Circuits Symposium, 535-538.

Nieminen H., Ermolov V., Silanto S., Nybergh K. and Ryhanen, T., 2004, Design of a temperature-stable RF MEM capacitor", IEEE Journal of Microelectromechanical Systems, 13: 705–714.

O'Mahony, C., Hill, M., Duane, R., and Mathewson, A., 2003, Analysis of Electromechanical Boundary Effects on the Pull-in of Micro-machined Fixed–Fixed Beams, Journal of Micromechanics and Microengineering, 13: 75–80.

Rebeiz, G.M., 2003, RF MEMS theory, design and technique, New York: John Wiley & Sons.

Sukomal Dey was born in 1982, India. He received his B.Tech degree in Electronics and communication engineering from state University, West Bengal, India in 2006. He completed his M.Tech degree in Mechatronics engineering from Bengal Engineering and Science University, Shibpur, India in 2009. He did a one year M.tech dissertation from Central electronics Engineering Research Institute (CEERI), Pilani. Presently he is doing a PhD at the Indian Institute of technology (IIT), Delhi. His research interests are in the area of RF-MEMS techniques for microwaves, and the application of micromachining for millimeter-wave circuits.

Shiban K Koul received a B.E. degree in Electrical Engineering from the Regional Engineering College, Srinagar in 1977, and M.Tech and PhD degrees in Microwave Engineering from the Indian Institute of Technology, Delhi, India in 1979 and 1983, respectively. He is a Professor at the Centre for Applied Research in Electronics where he is involved in teaching and research activities. His research interests include: RF MEMS, Device modeling, Millimeter wave IC design and Reconfigurable microwave circuits including antennas. He is currently the Deputy Director (Strategy and Planning) at the Indian Institute of Technology Delhi. He is also the Chairman of M/S Astra Microwave Pvt. Ltd, a major private company involved in the Development of RF and Microwave systems in India. He is author/co-author of 210 Research Papers and 7 state-of-the art books. He has successfully completed 25 major sponsored projects, 50 consultancy projects and 35 Technology Development Projects. He holds 7 patents and 4 copyrights.

Dr Koul is a Fellow of the IEEE, USA, Fellow of the Indian National Academy of Engineering (INAE) India and Fellow of the Institution of Electronics and Telecommunication Engineers (IETE) India, He has received a Gold Medal from the Institution of Electrical and Electronics Engineers Calcutta (1977); Indian National Science Academy (INSA) Young Scientist Award (1986); International Union of Radio Science (URSI) Young Scientist Award (1987); the top Invention Award (1991) of the National Research Development Council for his contributions to the indigenous development of ferrite phase shifter technology; VASVIK Award (1994) for the development of Ka- band components and phase shifters; Ram Lal Wadhwa Gold Medal (1995) from the Institution of Electronics and Communication Engineers (IETE); Academic Excellence award (1998) from the Indian Government for his pioneering contributions to phase control modules for the Rajendra Radar, Shri Om Prakash Bhasin Award (2009) in the field of Electronics and Information Technology, and a teaching excellence award (2012) from IIT Delhi.Dr. Koul is a distinguished IEEE Microwave Theory and Techniques Lecturer for the years 2012-2014.